Crisis in time-dependent dynamical systems

Simona Olmi[1, 2, *] and Antonio Politi[3, 1, †]

[1]*Istituto dei Sistemi Complessi, Consiglio Nazionale delle Ricerche,*
via Madonna del Piano 10, I-50019 Sesto Fiorentino, Italy
[2]*INFN, Sezione di Firenze, Via Sansone 1, I-50019 Sesto Fiorentino, Italy*
[3]*Institute for Complex Systems and Mathematical Biology University of Aberdeen, Aberdeen AB24 3UE, United Kingdom*

Many dynamical systems operate in a fluctuating environment. However, even in low-dimensional setups, transitions and bifurcations have not yet been fully understood. In this Letter we focus on crises, a sudden flooding of the phase space due to the crossing of the boundary of the basin of attraction. We find that crises occur also in non-autonomous systems although the underlying mechanism is more complex. We show that in the vicinity of the transition, the escape probability scales as $\exp[-\alpha(\ln \delta)^2]$, where δ is the distance from the critical point, while α is a model-dependent parameter. This prediction is tested and verified in a few different systems, including the Kuramoto model with inertia, where the crisis controls the loss of stability of a chimera state.

The study of forced dynamical systems has recently attracted much interest, since this setup allows analysing complex systems under the assumption that a given fraction of the degrees of freedom can be treated as an external noise-like drive. This is particularly useful in the context of global models of climate evolution, where the concept of "pull-back" attractors has been introduced precisely for this goal [1, 2]. Another research area where this simplification proves useful is synchronization of "slave" systems forced by a "master", especially in the presence of a dynamic control [3]. This includes the study of globally coupled oscillators, where the self-determined mean field can, in many respects, be treated as an external drive.

Within the more mathematically oriented community, these dynamical systems are identified as "non-autonomous". They undergo similar qualitative changes to those exhibited by (time) translationally invariant dynamical systems, when some control parameters are varied. However, they are complicate to analyse since the instantaneous configuration is not unique; it depends on the (typically unknown) configuration of the master (see [4] for a review).

In this Letter, we focus on a transition extensively investigated in chaotic low-dimensional systems: the "crisis", where the attractor reaches (and crosses) the boundary of its basin of attraction, suddenly widening the region of phase space explored by the stationary state [5]. A preliminary study of a crisis in forced systems has been performed in a model of El Niño-Southern Oscillation [6]. Here, we investigate this phenomenon in a context where a parameter fluctuates, being the result of an external nonlinear dynamical process. Crises in noisy dynamical systems had been extensively studied in the '90's of the previous century, but the analysis was always focused on theoretical estimates of the escape time in the vicinity of the deterministic critical point. The goal was achieved by expressing the dependence of the escape time on a single parameter: the ratio between the distance from the critical point and the noise amplitude (the latter one being

either unbounded as in [7–10], or bounded as in [11, 12]). Here, we show that under the assumption of bounded (not necessarily small) fluctuations, "noise" shifts the position of the transition point and induces an antirely new scaling behavior.

We first investigate the occurrence of a crisis with reference to the second-order Kuramoto model, commonly used for describing networks of oscillators capable of adjusting their natural frequencies. The inclusion of inertia induces a complex collective dynamics, where a fluctuating chimera state destabilizes via one such type of crisis. Numerical simulations reveal a strong divergence of the escape time, exhibited also by simplified models such as the modulated Hénon- and logistic-map. Thanks to a further simplification, we are able to derive analytical formulas, which are found to reproduce the behavior of various dynamical models.

Globally coupled Kuramoto rotors. Here we consider a network of N identical, symmetrically coupled rotators, each characterized by a phase ϑ_i and a frequency $\dot{\vartheta}_i$. The phase ϑ_i of the ith oscillator evolves according to the differential equation

$$m\ddot{\vartheta}_i(t) + \dot{\vartheta}_i(t) = \frac{K}{N} \sum_j^N \sin\left(\vartheta_j(t) - \vartheta_i(t) + \gamma\right), \quad (1)$$

where $m = 6$ is the inertia ($1/m$ plays the role of dissipation) and $\gamma = 1.6$ is a fixed phase lag. The oscillators are homogeneously coupled (we set $K = 6$, without loss of generality). Symmetry may spontaneously break, splitting the entire population in groups which exhibit a different behavior. Particularly interesting is the case when a *dust* of non synchronized units coexists with one or more *clusters* of perfectly synchronized oscillators. This regime, called chimera state, has been explored in several setups [13–20]; it emerges also in the Kuramoto model with inertia [21–23]. An exemplary chimera snapshot is presented in Fig. 1(a), where the empty black dots identify the dust (composed of 1214 oscillators), while the green square represents a cluster (composed of 786 oscil-

lators). Since all oscillators are identical, the stability of such regimes can be fruitfully investigated by focusing on the response of a single oscillator to a given mean field. This way, the problem is recognized as an instance of stability assessment of a time-dependent (non-autonomous) dynamical system. This is transparent once we rewrite the evolution equations in terms of the Kuramoto order parameter

$$R(t)e^{i\Phi(t)} = \frac{1}{N_d} \sum_{j=1}^{N_d} e^{i(\vartheta_j - \gamma)}, \qquad (2)$$

where N_d is the number of oscillators in the dust. The modulus $R(t) \in [0, 1]$ quantifies the degree of synchrony: in the continuum limit $R \approx 0$ means that the dust is distributed in an asynchronous state, while $R = 1$ implies a full phase synchronization. Under the assumption of a single cluster, Eq. (1) can be expressed as

$$m\ddot{\vartheta}_i + \dot{\vartheta}_i = K f_{cl} \sin(\Psi - \vartheta_i - \gamma) + K f_d R \sin(\Phi - \vartheta_i), \quad (3)$$

where Ψ is the phase of the cluster, while $f_{cl} \equiv 1 - f_d$ represents the fraction of oscillators therein. Eq. (3) describes the evolution of a modulated oscillator, the modulation being determined by the three time-dependent fields R, Φ and Ψ [24]. Depending on the initial condition, the oscillator may either: (i) collapse onto the cluster; (ii) converge towards the dust of unsynchronized oscillators. First-hand information on the stability of these two regimes can be extracted from the linearized equations,

$$m\delta\ddot{\vartheta} + \delta\dot{\vartheta} = -K [f_{cl} \cos(\Psi - \vartheta - \gamma) + f_d R \cos(\Phi - \vartheta)] \delta\vartheta, \qquad (4)$$

where we have dropped the no-longer necessary subindex i. Any stationary regime is characterized by two Lyapunov exponents: their sum is equal to $-1/m$, which quantifies the overall degree of dissipation. A stable cluster is identified by the presence of two negative Lyapunov exponents: this is the extension of a fixed point to the case of a time-dependent (non-autonomous) dynamical system. The dust, instead, is identified by one positive exponent: this is an instance of a time-dependent chaotic regime. In typical regimes, the positive exponent is approximately equal to 0.02.

Simulations show that a light dust (small f_d) does not self-sustain. In this regime, isolated clusters appear that are linearly unstable: they "emit" oscillators which are eventually absorbed by the dust itself.

For intermediate f_d values ($f_{cl} \gtrsim 0.5$), the chimera state is stationary: oscillators do neither migrate towards the dust, nor are they absorbed by the clusters. In this bistable regime, a probe oscillator, guided by the mean field without influencing it, may, depending on the initial condition, collapse onto either the dust or the cluster. The two basins of attraction are separated by the stable
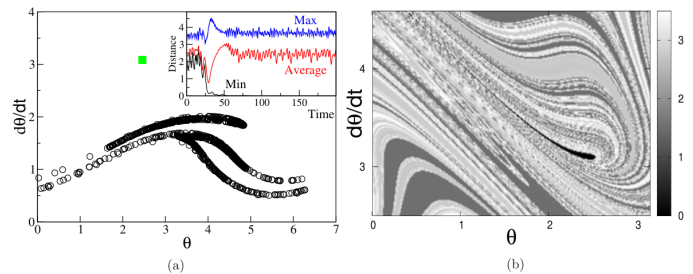

FIG. 1. (a) Snapshot of the Kuramoto model in the phase plane $(\dot{\vartheta}, \vartheta)$. The green square denotes the cluster position, while the open circles denote the dust. ($f_{cl} = 0.393$). Inset: time dependence of the dust-cluster distance in the presence of a migration event. The blue (red) curve identifies the maximal (average) Euclidean distance between the dust and the cluster. The black curve identifies the distance between the cluster and the nearest dust oscillator. Around t=100 the minimal distance virtually vanishes, indicating the occurrence of a migration event. (Initially, $f_{cl} = 0.465$.). (b) Basin of attraction of the cluster. The greyscale in $\mathbf{P} = (\vartheta, \dot{\vartheta})$ identifies the Euclidean distance of a probe oscillator (initially in $\mathbf{P}$) from the cluster after a time $t_e = 100$. Initial conditions are varied in a grid of size 0.01 in both directions. The cluster is initially in $(2.48160, 3.12)$ and $f_{cl} = 0.5$.

manifold of a second unstable cluster. While it is computationally hard to reconstruct directly this manifold which fluctuates, we can offer a glimpse of its structure, by proceeding as follows. An ensemble of probe oscillators is initialized inside a box encircling the cluster and let evolve for a long but finite time t_e. The final Euclidean distance between each probe oscillator and the cluster reveals a fractal intertwining of the two basins of attraction (see Fig. 1(b)).

By further increasing f_d, an intriguing instability sets in: oscillators sporadically leave the dust, eventually landing on a single cluster. One such episode is represented in the inset of Fig. 1(a), where we plot the evolution of the instantaneous Euclidean distance of the center of mass of the dust (red curve) together with the maximal (blue curve) and minimal (black curve) distance, from the cluster. There, we see a sudden approach of the dust to the cluster accompanied and followed by the loss of one (or more) oscillators. More quantitatively, there exists a critical fraction $\tilde{f}_d \approx 0.515$ above which the dust becomes metastable. Upon converging to $\tilde{f}_d$ from above, the escape rate from the dust progressively vanishes (see Fig. 2(a)). Altogether, this is the scenario of a crisis in a regime where the dust (the attractor undergoing the transition) is time dependent as well as its basin of attraction.

Simpler models. Now, we consider two stochastically-modulated systems, affected by a finite noise to simulate a deterministic chaotic forcing. The first model is the Hénon map, $y_{n+1} = a_n - y_n^2 + bx_n$, where the control parameter a_n is a uniformly distributed ($a_n \in [a - \Delta, a + \Delta]$)

δ-correlated noise. For $a = 1.4$, $b = 0.3$, and $\Delta = 0$ the map generates the standard Hénon attractor. If a is increased above $a_c = 1.42692111\ldots$, the invariant measure crosses the stable manifold of the fixed point $y^* = (b - 1 - \sqrt{(1-b)^2 + 4a})/2$, thereby escaping from the basin of attraction. This is a standard crisis. If we set $\Delta = 0.03$ and progressively increase a, the first escapes from the attractor occur for $a = 1.366$, i.e. when the maximum value is $a_{max} = 1.396$, below a_c. This means that the transition is not simply determined by the fluctuations above the critical value of the noiseless system. The dependence of the outgoing flux from the attractor on the parameter a can be appreciated in the inset of Fig. 2(a), where we see that the scenario is qualitatively very similar to that of the Kuramoto model (see the body of the same figure).

Next we analyse a yet simpler system: the logistic map, $x_{n+1} = a_n - x_n^2$. In the absence of fluctuations, the basin of attraction is the interval $[x^-, x^+]$, where $x^- \equiv (-1 - \sqrt{1+4a})/2$ is the negative fixed point, while $x^+ = a$ is the maximum of the map. Above $a_c = 2$, x^+ is mapped to the left of x^- so that the trajectory escapes to infinity.

If we let a_n fluctuate in the interval $[a - \Delta_c, a + \Delta_c]$, the escape can happen if the minimum possible value of x_n at time n (the iterate of the maximum a_{n-1} at the previous time) is smaller than the leftmost position of the fixed point x_n^- at time n. Mathematically,

$$ a - \Delta_c - (a + \Delta_c)^2 = \left(-1 - \sqrt{1 + 4(a - \Delta_c)} \right)/2 $$

where $\Delta_c(a)$ represents the minimal amplitude of the noise such that escapes from the attractor can occur. The curve is graphically plotted in Fig. 2(b) (green curve): there we see that in the limit $a = 2$, $\Delta_c = 0$, we recover the well known behavior of the deterministic logistic map. Interestingly, we also see that for $a < 2$ the maximum value of a ($a^+ = a + \Delta_c$) is always strictly smaller than 2 (see the Supplemental Material [25] for the complete derivation of the formula for a^+), showing that, analogously to the Hénon map, the presence of fluctuations lowers the critical point. This is evident when looking at the dashed blue curve, where $2 - a^+$ is plotted, in Fig. 2(b).

The average escape probability for $a = 1.95$, is reported in Fig. 2(d) versus $\delta = \Delta - \Delta_c$ ($\Delta_c = 0.01242$). The observed scaling behavior is explained in the next paragraph.

Scaling behavior. We start decomposing the dynamics around criticality into two regimes: (i) a standard chaotic phase (CP) in the bulk of the attractor; (ii) a grey zone (GZ) between the minimal and the maximal position of the "fixed" point x^- which may end up with either a final expulsion or a re-injection into the CP. This regime can also be seen as a stochastic motion in the vicinity of a random saddle. A linear stochastic model of the GZ dynamics suffices to determine the scaling behav-
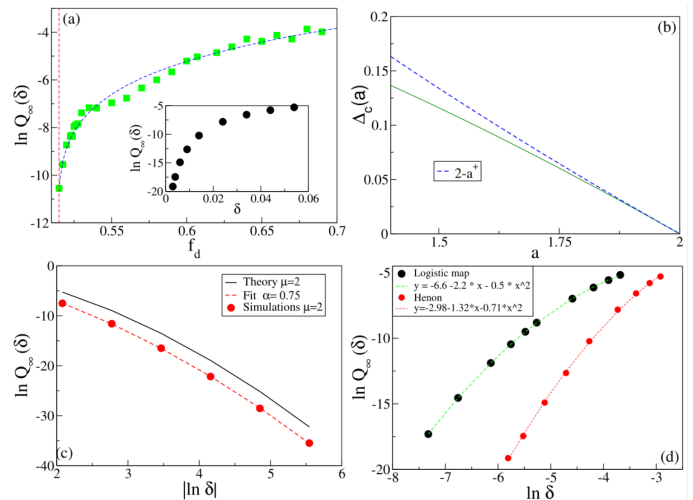

FIG. 2. (a) Kuramoto model: escape probability towards the cluster as a function of the initial value of f_d. Each value is obtained by averaging over 10 different realisations each of length $t = 2000000$. The dashed line is a fit with Eq. (10). In the inset, the escape probability vs the distance from the critical point is reported for the Hénon map. (b) Critical noise amplitude vs the average value of the parameter a for the logistic map. (c) Escape probability vs the logarithm of the distance from criticality for the linear stochastic model of the GZ dynamics. (d) Scaling behavior of the escape probability for the logistic and Hénon map. Black (red) dots represent simulation data for the logistic (Hénon) map, while the green (red) dashed line represent the corresponding scaling behavior estimated by following Eq. (7).

ior of the escape times. We assume that the phase point y_n obeys the following map,

$$ y_{n+1} = (y_n - \sigma_n)\mu + \sigma_n \ . \tag{5} $$

The iteration amounts to an expansion by a factor μ of the current distance of y_n from a randomly selected unstable "fixed" point $\sigma_n \in [0,1]$ (this mimicks the fluctuations of a_n). The GZ is the unit interval $[0,1]$, and the initial condition y_1 is uniformly distributed within $[1 - \delta, 1]$, where δ represents the distance from criticality. Finally, a trajectory terminates when either $y_n < 0$, meaning that the point is unavoidably expelled from the former attractor, or $y_n > 1$, meaning that it is reinjected in the bulk.

The probability density $P_n(y)$ to lie in $[y, y + dy]$ at time n satisfies the Frobenius-Perron equation

$$ P_{n+1}(y) = \frac{1}{\mu} \int_0^1 d\sigma P_n[y/\mu + \sigma(1 - 1/\mu)] \ . \tag{6} $$

Hence, the probability to escape from the attractor within the first n iterates is

$$ Q_n(\delta) = \sum_{k=1}^{n} \int_{1-\mu}^{0} P_k(y) dy $$

where the lower limit of the integral is the minimum attainable y-value (as from Eq. (5)). We are interested in $Q_\infty(\delta)$. It is obvious that $Q_\infty(\delta) < Q_n(\delta) + G_n(\delta)$, where

$$G_n(\delta) = \int_0^1 P_n(y)dy \qquad (7)$$

denotes the probability to be in the GZ after n iterates.

A trajectory starting close to 1 cannot initially escape on the left, no matter the values taken by σ_n. It can do so, only after M iterates when $\mu^M\delta \geq 1$. Equivalently, $Q_n = 0$ for $n \leq M = -\ln\delta/\ln\mu$ and we can conclude that $Q_\infty(\delta) < G_M(\delta)$.

Interestingly, P_n (and G_n) can be analytically estimated for $n \leq M$. It can indeed be verified (see [25]) that

$$P_n(y) = K_n(y - 1 + \mu^n\delta)^n \qquad y \geq 1 - \mu^n\delta \quad (8)$$

and is zero otherwise, where

$$K_{n+1} = \frac{K_n}{\mu - 1}\frac{1}{(n+1)\mu^{n+1}}.$$

By solving this recursive relation for the initial condition $K_0 = 1/\delta$, we obtain

$$K_n = \left[\delta(\mu-1)^n n! \mu^{n(n+1)/2}\right]^{-1}.$$

In virtue of Eq. (8), the probability $G_n(\delta)$ is therefore (for $n \leq M$)

$$G_n(\delta) = K_n \int_{1-\mu^n\delta}^1 dy(y-1+\mu^n\delta)^n = \frac{K_n(\mu^n\delta)^{n+1}}{n+1}$$

so that

$$G_n(\delta) = \left(\frac{\delta}{\mu-1}\right)^n \frac{\mu^{n(n+1)/2}}{(n+1)!}. \qquad (9)$$

By invoking the Stirling approximation

$$G_n \approx \exp\left[n\ln\delta - n\ln\mu + \frac{n(n+1)}{2}\ln\mu - n\ln n + n\right]$$

and setting $n = M = -\ln\delta/\ln\mu$, we find that up to the first two leading terms in δ

$$G_M \approx \exp\left[-\alpha(\ln\delta)^2 + \beta\ln\delta\right] \qquad (10)$$

where $\alpha = 1/(2\ln\mu)$. $G_M(\delta)$ is an upper bound of $Q_\infty(\delta)$. Its decrease with δ is slower than exponential but faster than any power law.

In Fig. 2(c), we can compare the theoretical prediction (10) (black curve) with the direct values of $Q_\infty(\delta)$ (red dots), for $\mu = 2$. Obviously, $Q_\infty < G_M$. Since the gap between the two quantities does not increase upon decreasing δ, we can conjecture that G_M, i.e. the probability to be still in the GZ when it becomes possible at
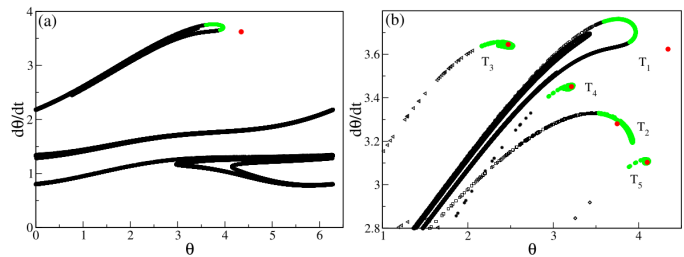

FIG. 3. (a) Snapshot of the Kuramoto model in the phase plane $(\vartheta, \dot\vartheta)$. The red dot corresponds to the cluster position, while the black and green circles correspond to the dust. (initially, $f_{cl} = 0.393$). (b) Enlargement of panel (a) around the cluster position corresponding to the evolution at time T_1. Here are reported enlargements of the same dynamical evolution for successive times $T_2, .., T_5$ (identifiable by different symbols) to characterize the tunnel zone in the cluster growth problem.

all to escape on the left, represents the leading contribution to $Q_\infty(\delta)$ (for $\delta \to \infty$). In fact, by using α and β as fitting parameters, Eq. (10) provides a very good reproduction of the numerical data: see the dashed line in Fig. 2(c), obtained for $\alpha \approx 0.75$, to be compared with the theoretical expectation for G_M: $1/(2\ln 2) = 0.721\ldots$.

Back to dynamical models. Now, we go back to the logistic map. In Fig. 2(d) we report the data so as to emphasize the quadratic dependence on $\ln\delta$ (see full black dots). A fit in terms of Eq. (10) (with α and β as free parameters) reproduces very well the numerical observations, although now $\alpha \approx 0.5$ differs more from the theoretical expectation (≈ 0.4), the reason being that the quadratic maximum of the logistic map induces a singularity in the distribution of initial conditions in the GZ, which is not taken into account in the theory. In Fig. 2(d) we report also the data for the Hénon map (full red dots): the quality of the fit is again very good, in spite of the two-dimensional character of the phase space. Hence, the GZ is not an interval containing fluctuating saddle; it is a thin corridor covering its stable manifold. Nevertheless, in the small δ limit, the scenario is similar, since the relevant trajectories naturally flow towards the saddle point (observational evidence is offered in [25]).

Finally, we go back to the Kuramoto model. Here, the collapse onto the cluster is equivalent to the divergence observed in the logistic map. The single-oscillator dynamics is two-dimensional as in the Hénon map, but now the external modulation plays a double role: it induces a chaotic dynamics (otherwise impossible in a two-dimensional continuous-time, autonomous dynamical system) testified by the fractal basin boundary (as visible in Fig. 1(b)) and is responsible for the stochastic-like fluctuations of the basin boundary: it is, in fact, well known that mean-field type models may be characterized by a high- (actually infinite-) dimensional dynamics (see Ref. [26] and references therein). Evidence of the

pseudo-random oscillations of the order parameter in the second-order Kuramoto is given in [25].

The direct reconstruction of the GZ is computationally hard, but we can illustrate an escape event. In Fig. 3, we show four different instances of the distribution of points in correspondence of the escape of some oscillators from the cloud (10^6 probe oscillators have been added to make the scenario clear). A "tongue" is initially emitted out by the dust (as a consequence of some fluctuation); the tip of the tongue reaches the cluster, while the rest pulls back. The points in the tongue can be interpreted as belonging to the GZ; some of them (green) eventually leave the attractor (the dust), while others (black) ones are pushed back to the dust. Quantitatively, the numerical values of the escape rate have been fitted with the theoretical expression Eq. (10). The outcome, reported in Fig. 2(a) (see the dashed line, which corresponds to $\alpha = 0.13$), reveals again excellent agreement with the raw data.

Conclusions. We have shown that the crisis, a typical transition occurring in chaotic attractors, may also arise in time-dependent models, although the scaling behavior is very different and the mechanism itself is more complicate since it is controlled by a tunnelling mechanism induced by the fluctuations of the underlying basin of attraction. How to determine α? In the simple stochastic one-dimensional model, it is linked to the instability of the fixed point whose stable manifold determines the boundary of the basin of attraction. More in general, we can imagine that the fractal dimension of the attractor to enter as well and the correlations probably play a crucial role. This is left to future work.

* simona.olmi@cnr.it
† a.politi@abdn.ac.uk

[1] H. Crauel and P. E. Kloeden, Jahresber. Dtsch. Math. Ver. 117, 173-206 (2015).
[2] S. Pierini, M. D. Chekroun, and M. Ghil, Nonlinear Processes in Geophysics 25, 671–692 (2018).
[3] J. Pena Ramirez, A. Arellano-Delgado, and H. Nijmeijer, Phys. Rev. E 98, 012208 (2018).
[4] P. T. Clemson and A. Stefanovska, Phys. Rep. 542, 297 (2014).
[5] C. Grebogi, E. Ott, and J. A. Yorke, Phys. Rev. Lett. 48, 1507 (1982).
[6] M. D. Chekroun, M. Ghil, and J. D. Neelin, in *Advances in nonlinear geosciences*, edited by A. A. Tsonis (Springer International Publishing, 2018) pp. 1,33.
[7] J. C. Sommerer, E. Ott, and C. Grebogi, Phys. Rev. A 43, 1754 (1991).
[8] J. C. Sommerer, W. L. Ditto, C. Grebogi, E. Ott, and M. L. Spano, Phys. Rev. Lett. 66, 1947 (1991).
[9] M. Franaszek, Phys. Rev. A, 44(6), 4065.
[10] P. Reimann, J. Stat. Phys., 82, 1467-1501 (1996).
[11] P. Reimann, J. Stat. Phys., 85, 403-425 (1996).
[12] R. Wackerbauer, Phys. Rev. E, 59(3), 2872 (1999).
[13] Y. Kuramoto and D. Battogtokh, arXiv preprint cond-mat/0210694 (2002).
[14] D. M. Abrams and S. H. Strogatz, Phys. Rev. Lett. 93, 174102 (2004).
[15] O. E. Omelchenko, Y. L. Maistrenko, and P. A. Tass, Phys. Rev. Lett. 100, 044105 (2008).
[16] A. Pikovsky and M. Rosenblum, Phys. Rev. Lett. 101, 264103 (2008).
[17] C. R. Laing, Chaos: An Interdisciplinary Journal of Nonlinear Science 19 (2009).
[18] S. Olmi, A. Politi, and A. Torcini, EPL 92, 60007 (2011).
[19] E. Schöll, The European Physical Journal Special Topics 225, 891 (2016).
[20] A. Zakharova, *Chimera patterns in networks* (Springer, 2020).
[21] P. Jaros, Y. Maistrenko, and T. Kapitaniak, Phys. Rev. E 91, 022907 (2015).
[22] S. Olmi, E. A. Martens, S. Thutupalli, and A. Torcini, Phys. Rev. E 92, 030901(R) (2015).
[23] S. Olmi, Chaos: An Interdisciplinary Journal of Nonlinear Science 25 (2015).
[24] Ψ satisfies Eq. (3), in which case, the argument of the first sinusoidal term reduces to $-\gamma$.
[25] See Supplemental Materials for details on the simpler models and high-dimensional chaotic dynamics in Kuramoto oscillators, which includes Refs. [27, 28].
[26] A. Politi, A. Pikovsky, and E. Ullner, Eur. Phys. J. Special Topics 226, 1791 (2017).
[27] G. Benettin, L. Galgani, A. Giorgilli, and J.-M. Strelcyn, *Meccanica* 15, 9 (1980).
[28] A. Pikovsky and A. Politi, *Lyapunov exponents: a tool to explore complex dynamics*, Cambridge University Press (2016).